Modeling the slippage between membrane and border cables

Ruy M.O. PAULETTI*, Carolina B. MARTINS

*Polytechnic School, University of São Paulo
P.O. Box 61548, 05424-970 São Paulo, Brazil
pauletti@usp.br

Abstract

This paper presents the theoretical formulation and the implementation of a class of finite elements capable of representing the slippage between border cables and membrane sheaths, without distortion of the cable's tangent stiffness. After reviewing the *3-node* Aufare's *sliding-cable element*, new *sliding-cable super-element* is proposed, which simplifies the mesh generation labor and overcomes some limitations of Aufare's elements to deal with large amounts of relative sliding between cables and membrane, which arises as long as meshes are refined.

Keywords: border cables, sliding, membrane structures, nonlinear analysis.

1. Introduction

Programs aimed to the analysis of membrane structures, usually by means of the finite element method (FEM), very seldom have at hand some element which can represent satisfactory, and without high computational costs, the slippage between a cable and the membrane it is devised to restrain. Modeling the cable as a sequence of no-compression truss elements is usual in engineering practice. However, that implies in perfect adherence between cable and membrane, which is seldom the case, if ever. This feature is not problematic during the phase of shape finding of the membrane, since shape finding is an essentially immaterial process. But it does distort the response of the actual, material membrane, under service loads.

This paper is restricted to the study of cases when the cable is transversally constrained by the membrane surface, in such a way that sliding is only possible tangentially to the cable development. This is the case of the cables commonly used along the membranes borders, as well as of the internal ridge or valley cables used to fold and strengthen a membrane. We will refer to all of these cables, generically, as "border cables".

For small to medium size structures, when the cable diameters are small and the fabrics more flexible, a practical solution to transfer the transversal loads from the membrane to the border cables is the use of sheaths, welded or sewn directly to the membrane fabric, as shown in Figure 1(a). For larger spans, such as in Denver's Airport, less flexible fiberglass fabrics and larger cable diameters are required, so the border cables are positioned externally to the membrane. Stresses in the membrane, transversal to the border, are transferred to the external border cables through a system of plates which are compressed against the upper and lower surfaces by a series of bolts. Polymeric strips are inserted between the membrane and the plates, to reduce the friction between the contact surfaces and avoid wearing of the fabric. The membrane is made thicker at the border, and the resulting interference restrains the membrane from slipping inwards, and the plates from slipping outwards. From the border plates, loads are transferred to the external cable by means of clamps, as shown in Figure 1(b/c).
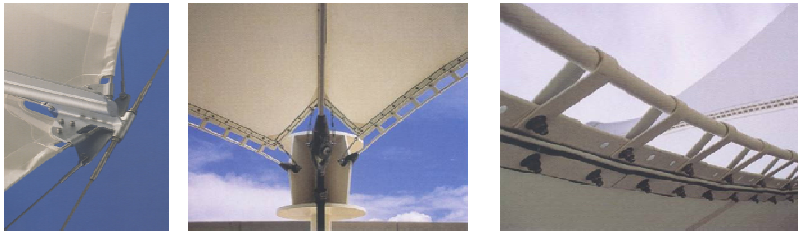

Figure 1: (a) border cables inside sheaths; (b/c) border cables of Denver's Airport [1].

2. Modeling border cables

According to [2], the problem of the slippage of cables over a membrane had been noticed by several researchers [3],[4],[5], but has not yet been solved completely. As reviewed by [5], Matsumura [3] was the first to cope with the sliding problem in membrane structures, introducing a sort of "bending" elements into the analysis.

A crude frictionless slippage analysis could simply assume the cable as a chain of truss elements with a very flexible material, under high initial strains, in such a way that the normal load on the cable would remained practically unaltered by the structure's deformation. That indeed provide a good approximation to structures where the cables' stiffness can be disregarded, such as in post-tensioned concrete members, when cables sometimes are even treated as an external distributed load. Nevertheless, in the case of membrane structures, the stiffness of the cables usually surpasses the membrane stiffness, and disregarding this feature can alter the structure's equilibrium configuration and internal stress state.

A general way to simulate the slippage between border cables and membranes is the development of a contact analysis. However, inclusion of contact elements between cables and membrane is a cumbersome process, and contact analyses usually require a large computational effort. On this line, an interesting model to study the behavior of a stabilizing cable laid over the surface of the membrane, using surface-based contact elements available in a commercial program based on the FEM was presented in [2].

However, in the context of the FEM, analysis of problems such as the folding of a membrane by a cable sliding over it in a generic way requires very refined, adaptive meshes. To overcome this limitation, a mesh-free method, based on the element free Galerkin (EFG) method, was presented in [6], yielding satisfactory results in the representation of both sliding and creasing.

In the case of border cables, where the cables are transversally restrained, and slippage can only occurs if tangent to the cable, a less expensive way to model the phenomenon is offered by the sliding-cable element first proposed by Aufare [7], in the context of the cables of transmission lines. Aufare's element was subsequently generalized by Pauletti [8],[9], considering the influence of dry friction. The element was successfully employed to model non-adherent tendons of post-tensioned concrete structures [10], as well as the hoisting of tensegrity domes [11]. The possibility of employing this element to model border cables had already been advanced by [8], but the task was postponed until the current paper.

Even though Aufare's element is capable of modeling problems involving border cables, it requires definition of extra nodes, not belonging to the membrane mesh, to connect several sliding cables into a larger chain. Now, since this element collapses if the intermediate, "pulley" node slides until touching one of the end nodes, the maximum allowed slippage diminishes, as long as the mesh is refined. This is a serious nuisance, since a slippage analysis will probably be required precisely when concern about stress concentrations exists, and refined meshes become most necessary. These drawbacks were the main motivation to the development of the *sliding-cable super-element* discussed ahead.

A brief survey of literature reveals that elements similar to the sliding-cable super-element proposed in this paper have been already considered by other authors. Mitsugi [12] presented a static analysis of cable networks and their supporting structures, proposing a "hyper-cable" element, with a variable number of nodes and basically the same material and kinematic hypothesis than the present paper. Also Zhou [13] has presented a sliding cable element consisting of a "string of cables that dynamically passes through a prescribed node, called the slider point, which can be either still or moving", in practice an assemblage of one Aufare's and several other truss elements.

3. Geometrically non-linear equilibrium

Assume that the nodal coordinates of a discrete system, $\mathbf{x}_i = \left[\vec{x}_i \right]_{3 \times 1}$, $i = 1, \ldots, n$, are stored in a *global position vector* $\mathbf{x} = \left[\mathbf{x}_1^T \quad \mathbf{x}_2^T \quad \ldots \quad \mathbf{x}_n^T \right]_{3n \times 1}^T$ (note that double-transpose of vectors is used to avoid a column-wise representation). Dealing with cables and membranes, assume that each node has only displacement degrees-of-freedom $\mathbf{u}_i = \left[\vec{u}_i \right]_{3 \times 1}$, $i = 1, \ldots, n$, stored in a *global displacement vector* $\mathbf{u} = \left[\mathbf{u}_1^T \quad \mathbf{u}_2^T \quad \ldots \quad \mathbf{u}_n^T \right]_{3n \times 1}^T$. The external loads acting on these nodes are stored in a *global external load vector* $\mathbf{F}$, and the nodal force interactions are stored in a *global internal load vector* $\mathbf{P}$ (with definitions analogous to $\mathbf{x}$ and $\mathbf{u}$). The position vector can be written as $\mathbf{x} = \mathbf{x}^0 + \mathbf{u}$, where $\mathbf{x}^0$ is a constant vector which describes

an initial configuration.

With the above definitions, the problem of finding the equilibrium configuration of a network of central forces can be posed as: "find $\mathbf{u}^*$ such that $\mathbf{g}(\mathbf{u}^*) = \mathbf{P}(\mathbf{u}^*) - \mathbf{F}(\mathbf{u}^*) = \mathbf{0}$ ", where $\mathbf{g}(\mathbf{u})$ is the *unbalanced load vector* (or "*error vector*").

This problem can be solved –within a vicinity of the solution– iterating Newton's recurrence formula,

$$\mathbf{u}_{i+1} = \mathbf{u}_i - \left(\frac{\partial \mathbf{g}}{\partial \mathbf{u}}\bigg|_{\mathbf{u}_i}\right)^{-1} \mathbf{g}(\mathbf{u}_i) = \mathbf{u}_i - \left(\mathbf{K}_t^{\,i}\right)^{-1} \mathbf{g}(\mathbf{u}_i), \qquad (1)$$

where the *tangent stiffness matrix* $\mathbf{K}_t^{\,i}$ is defined.

It is sometimes convenient to decompose the vector of internal forces as $\mathbf{P} = \mathbf{CN}$, where $\mathbf{N} = \mathbf{N}(\mathbf{u})$ is a vector of *scalar internal loads* and $\mathbf{C} = \mathbf{C}(\mathbf{u})$ is a *geometric operator*. There results, for the tangent stiffness matrix:

$$\mathbf{K}_t = \frac{\partial \mathbf{g}}{\partial \mathbf{u}} = \frac{\partial}{\partial \mathbf{u}}(\mathbf{CN} \text{-} \mathbf{F}) = \mathbf{N}^T \frac{\partial \mathbf{C}}{\partial \mathbf{u}} + \mathbf{C}\frac{\partial \mathbf{N}}{\partial \mathbf{u}} - \frac{\partial \mathbf{F}}{\partial \mathbf{u}} = \mathbf{K}_g + \mathbf{K}_c + \mathbf{K}_{ext} \qquad (2)$$

where the *geometric*, the *constitutive* and the *external stiffness matrices* are respectively defined. It may be also convenient to define an *internal tangent stiffness matrix* $\mathbf{K}_{\text{int}} = \mathbf{K}_g + \mathbf{K}_c$. An interpretation of these stiffness components is given in [14] and [15].

It is not computationally convenient to calculate directly the structure's global stiffness matrix. Instead, the stiffness is calculated for each structural element and then added to the global stiffness matrix. So proceeding, the vector of the nodal displacements of the eth element is written as $\mathbf{u}^e = \mathbf{A}^e \mathbf{u}$, where $\mathbf{A}^e$ is a Boolean *incidence matrix* of that element, which also appears in the relationship between the element and the global internal load vectors, as well as in the relationship between the element and the global tangent stiffness matrices, according to

$$\mathbf{P} = \sum_{e=1}^{b} \mathbf{A}^{eT} \mathbf{p}^e \quad \text{and} \quad \mathbf{K}_t = \sum_{e=1}^{b} \mathbf{A}^{eT} \mathbf{k}_t^e \mathbf{A}^e \qquad (3)$$

Of course, it is not convenient to perform the matrix multiplications presented in (3), being quite more economical to add the element contributions directly to the global internal load vector and the tangent stiffness matrix, as explained in standard FEM textbooks.

4. Aufare's sliding-cable element

Figure 3(a) shows a cable passing throw a frictionless pulley. It can be shown that the problem is independent of the pulley radius, and thus the situation can be well represented

by an Aufare's element, in which the intermediate node is allowed to slide along the element length, as shown in Figure 3(b). Since no friction is considered, the normal load is constant in both straight segments into which the cable is divided, and $\vec{P}_3$ is directed along the bissetrix of the angle between them.
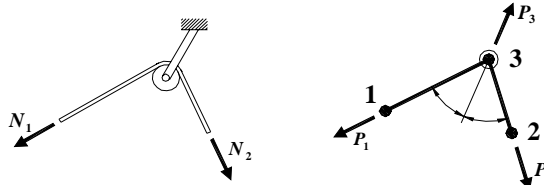

Figure 3: (a) a cable passing through a pulley; (b) an Aufare's sliding-cable element.

Keeping implicit the element index e, the total length of the cable, in the current configuration, is given by the addition of the lengths of the two segments, $\ell = \left(\mathbf{l}_1^T \mathbf{l}_1\right)^{\frac{1}{2}} + \left(\mathbf{l}_2^T \mathbf{l}_2\right)^{\frac{1}{2}}$, where $\mathbf{l}_1 = \mathbf{x}_1^0 + \mathbf{u}_1 - \mathbf{x}_3^0 - \mathbf{u}_3$ and $\mathbf{l}_2 = \mathbf{x}_2^0 + \mathbf{u}_2 - \mathbf{x}_3^0 - \mathbf{u}_3$. The element is defined in an initial configuration, already subject to a normal force N^0. The initial length ℓ_0 is obtained from $\mathbf{l}_1^0 = \mathbf{x}_1^0 - \mathbf{x}_3^0$ and $\mathbf{l}_2^0 = \mathbf{x}_2^0 - \mathbf{x}_3^0$. The stress-free, reference length, considering linear-elastic behavior is given by $\ell_r = EA\ell_0 / \left(EA + N_0\right)$, and thus the normal load in the current configuration is $N = EA\left(\ell - \ell_r\right) / \ell_r$.

The displacement and internal forces vectors are given, respectively, by

$$\mathbf{u} = \begin{bmatrix} \mathbf{u}_1 \\ \mathbf{u}_2 \\ \mathbf{u}_3 \end{bmatrix} \text{ and } \mathbf{p} = \begin{bmatrix} \mathbf{p}_1 \\ \mathbf{p}_2 \\ \mathbf{p}_3 \end{bmatrix} = \begin{bmatrix} \mathbf{v}_1 \\ \mathbf{v}_2 \\ -\left(\mathbf{v}_1 + \mathbf{v}_2\right) \end{bmatrix} N = \mathbf{C} N , \qquad (4)$$

where the normal load N is uniform along the element, $\mathbf{v}_1$ e $\mathbf{v}_2$ are unit vectors directed from node 3 to nodes 1 and 2, respectively, and matrix $\mathbf{C}$ is a geometric operator.

Deriving the vector of internal forces with respect to displacements, the internal tangent stiffness matrix is obtained, after some algebra. Denoting $\mathbf{M}_{ij} = \mathbf{v}_i \mathbf{v}_j^T$ and $\mathbf{M}_i = \mathbf{I}_3 - \mathbf{v}_i \mathbf{v}_i^T$, $i = 1, 2$, there results, for the elastic constitutive component of the tangent stiffness:

$$\mathbf{k}_e = \frac{EA}{\ell_r} \mathbf{CC}^T = \frac{EA}{\ell_r} \begin{bmatrix} \mathbf{M}_{11} & \mathbf{M}_{12} & -\left(\mathbf{M}_{11} + \mathbf{M}_{12}\right) \\ \mathbf{M}_{21} & \mathbf{M}_{22} & -\left(\mathbf{M}_{21} + \mathbf{M}_{22}\right) \\ -\left(\mathbf{M}_{11} + \mathbf{M}_{21}\right) & -\left(\mathbf{M}_{12} + \mathbf{M}_{22}\right) & \left(\mathbf{M}_{11} + \mathbf{M}_{12} + \mathbf{M}_{21} + \mathbf{M}_{22}\right) \end{bmatrix} \qquad (5)$$

and for the geometric component:

$$\mathbf{k}_g = \begin{bmatrix} \dfrac{N}{\ell_1}\mathbf{M}_1 & \mathbf{0} & -\dfrac{N}{\ell_1}\mathbf{M}_1 \\[2ex] \mathbf{0} & \dfrac{N}{\ell_2}\mathbf{M}_2 & -\dfrac{N}{\ell_2}\mathbf{M}_2 \\[2ex] -\dfrac{N}{\ell_1}\mathbf{M}_1 & -\dfrac{N}{\ell_2}\mathbf{M}_2 & \left(\dfrac{N}{\ell_1}\mathbf{M}_1 + \dfrac{N}{\ell_2}\mathbf{M}_2\right) \end{bmatrix} \tag{6}$$

It is seen that $\mathbf{k}_{\text{int}} = \mathbf{k}_e + \mathbf{k}_g$ is symmetric, as required for a conservative system.

Application of Aufare's element requires some caution, since the element collapses if the intermediate node coincides with one of the end nodes, and the intermediate node becomes hypostatic if the element rectifies and no further stiffness is provided to the node by other elements. A discussion on some actual and apparent singularities, as well as some elementary tests on this sliding-cable element, was presented in [8]. Pauletti [15],[16] presented also the matrices for the case of non-ideal, dry-friction sliding. In that case, due to friction, $\mathbf{k}_{\text{int}}$ looses symmetry. Aufare [17] also proposed another non-conservative sliding-camp/cable element, which ensures the continuity of the horizontal component of the internal forces at the sliding node.

A chain of several Aufare´s elements can be used to model the ideal sliding between a border cable and a membrane, but modeling becomes quite laborious, because many extra nodes are required, besides those representing the membrane, since only the intermediate node of each element is able to represent the slippage over the rest of the structure. Furthermore, mesh refinement is constrained by the amount of sliding that the cable undergoes since, as long as the elements becomes smaller, they may collapse with a smaller amount of slippage.

4. An ideal sliding-cable super-element

In order to circumvent the above mentioned problems, we propose an ideal (frictionless) *sliding-cable super-element,* shown in Figure 4, which simplifies the labor associated to mesh generation, since it does not require definition of any extra nodes, and which does not resent from the collapse of the intermediate nodes (when properly attached to membrane elements), so that any amount of relative sliding may be considered, regardless the level of mesh refinement.

The stiffness matrix of the new element could actually be obtained by static condensation of the degrees of freedom associated to the end nodes of each sliding-cable element, in such a way that only the intermediate, "pulley nodes" remains, thus the "super-element" nomenclature adopted in this work.
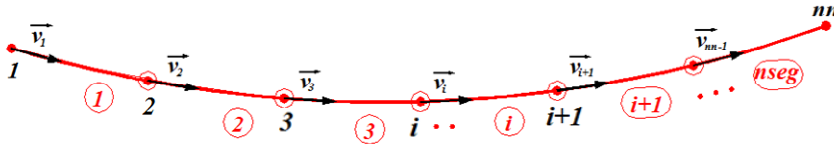
Figure 4: A super-element with n nodes and $n_{seg}=n-1$ segments, sliding over $n_p=n-2$ pulleys.

Associated to each segment $k=1,...,n_{seg}$ we obtain a vector $\mathbf{l}_k = \mathbf{x}_{k+1}^0 + \mathbf{u}_{k+1} - \mathbf{x}_k^0 - \mathbf{u}_k$, and the total current cable length is given by $\ell = \sum_{k=1}^{n_{seg}} \ell_k = \sum_{k=1}^{n_{seg}} \|\mathbf{l}_k\|$. The element is defined in an initial configuration, already under a normal force N_0, uniform along the cable, since ideal sliding is assumed. Defining $\mathbf{l}_k^0 = \mathbf{x}_{k+1}^0 - \mathbf{x}_k^0$, the cable length at the initial configuration is once again given by $\ell_0 = \sum_{k=1}^{n_{seg}} \|\mathbf{l}_0\|$. For a linear-elastic material, the total undeformed, reference cable length is $\ell_r = EA\ell_0 / (EA + N_0)$ and the normal load at the current configuration is $N = EA(\ell - \ell_r)/\ell_r$.

The inner loads acting on the nodes $i=1,...,n$ of the super-element, at the current configuration, are $\mathbf{p}_i = N(\mathbf{v}_{i-1} - \mathbf{v}_i)$, where $\mathbf{v}_i = \mathbf{l}_i / \ell_i$. Further defining $\mathbf{v}_0 = \mathbf{v}_n = \mathbf{0}$, the vector of nodal displacements and the vector of inner nodal loads of the element are given by

$$\mathbf{u} = \begin{bmatrix} \mathbf{u}_1 \\ \vdots \\ \mathbf{u}_i \\ \vdots \\ \mathbf{u}_n \end{bmatrix} \quad \text{and} \quad \mathbf{p} = \begin{bmatrix} \mathbf{p}_1 \\ \vdots \\ \mathbf{p}_i \\ \vdots \\ \mathbf{p}_n \end{bmatrix} = \begin{bmatrix} \mathbf{v}_0 - \mathbf{v}_1 \\ \vdots \\ \mathbf{v}_{i-1} - \mathbf{v}_i \\ \vdots \\ \mathbf{v}_{n-1} - \mathbf{v}_n \end{bmatrix} N = \mathbf{C}N \tag{7}$$

where $\mathbf{C}$ is a matrix geometric operator of order ($3n$ x 1).

After some straightforward derivations, we arrive at the elastic component of the tangent stiffness matrix, given by

$$\mathbf{k}_e = \frac{EA}{\ell_r} \mathbf{C}\mathbf{C}^T . \tag{8}$$

This is formally the same expression as in the case of Aufare's three-node element, equation (5). Nevertheless, contrary to a cable modeled as a chain of Aufare's elements, which requires additional degrees of freedom, yielding a $(2n-1)\times(2n-1)$ sparse-banded matrix, in the case of a sliding cable super-element, $\mathbf{k}_e$ is a full $n \times n$ symmetric matrix.

Other straightforward derivations provides the geometric stiffness matrix as a tri-diagonal assembling of order *3* x *3* nodal stiffness sub-matrices, $\mathbf{k}_g = \begin{bmatrix} \mathbf{k}_{ij} \end{bmatrix}$, $i,j = 1,...,n$, such that, for the ith line,

$$\mathbf{k}_{i,i-1} = -N\frac{\mathbf{M}_{i-1}}{\ell_{i-1}} \quad ; \quad \mathbf{k}_{ii} = N\left(\frac{\mathbf{M}_{i-1}}{\ell_{i-1}} + \frac{\mathbf{M}_i}{\ell_i}\right) \quad ; \quad \mathbf{k}_{i,i+1} = -N\frac{\mathbf{M}_i}{\ell_i} \tag{9}$$

Martins [18] compared the performance of the sliding-cable super-element with equivalent chains of Aufare's element in several benchmarks, concluding that both alternatives yield the same numerical results, with super-elements providing an easier mesh definition.

5. Application

As an application, we investigate the influence of the slippage of the border cables in the response of the membrane roof of the "*Memorial dos Povos de Belém do Pará*", shown in Figure 7. An account on the design and construction of this 400m^2 membrane, located at the main city of the State of Pará, Brazil is given in [19]. Discussions about the shape-finding and the patterning of this structure, as well as the residual stresses intrinsic to simple-to-double-curvature mappings involved, are given in [15] and [19].

In the present work, we investigate the response of a rough model of the MPBP under a uniform upward wind load $q = 286N/m^2$ acting over the whole membrane surface. All analyses were started from the same configuration, as determined in the phase of shape finding. The model had 120 nodes and 196 membrane elements, and the six vertices of the membrane were assumed to be fixed.

Figure 6: The membrane roof of the "Memorial dos Povos de Belém do Pará"

The study compared the response of the membrane bounded by six frictionless sliding border cables, each of them represented by one super-element (the "ideal-sliding model"), with the response of the membrane bounded by six fully adherent border cables, modeled with standard no-compression truss elements (the "fully-adherent model"). The membrane was modeled by Argyris' natural elements [20],[14],[15]. Akitas' model for handling wrinkling, via a matrix projection technique [21], was also implemented, and will be the object of a forthcoming paper.

Results obtained by the SATS program [14], via Newton's iterations, for both the "ideal-sliding" and the "fully-adherent" models, were compared to results obtained for the same problem, solved in SATS via dynamic relaxation (as described in [22]). Results for the

"fully-adherent" model were also compared with results given by the Ansys FEM code. A sliding cable is not directly available in Ansys, thus the sliding condition was not analyzed by that program.
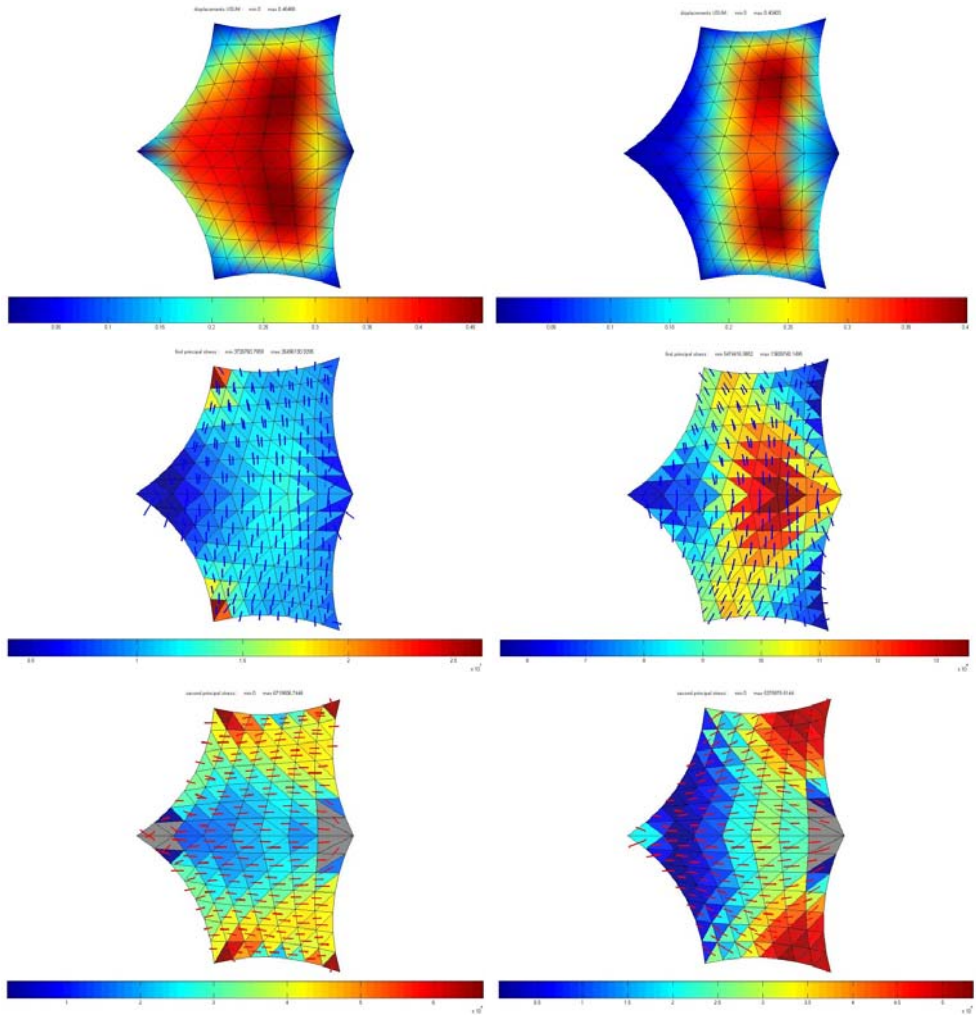

Figure 7: 1st column: ideal-sliding model; 2nd column: fully-adherent model.
1st row: displacement norms; 2nd row: 1st principal stresses σ_I; 3rd row: 2nd principal stresses σ_{II}, with wrinkled elements ($\sigma_{II} = 0$) shown in grey.

Table 1 compares some selected results obtained with both the ideal-sliding and the fully-adherent models. All results presented very good agreement. The wrinkled elements detected in SATS, in the fully-adherent model, presented very low but still positive 2nd principal stresses ($0 < \sigma_{II} < 8 \cdot 10^{-4}\,MPa$), in the corresponding Ansys model.

From the analysis of the results presented in Table 1 and Figures 7 and 8, it can be seen that consideration of sliding provokes an increase of only about 10% in maximum membrane displacements, but doubles the maximum first principle stresses σ_I.

Thus, little as may be the influence of cable slippage on the overall membrane configuration, it still can introduce regions of high stress concentrations, from which an overall structural failure can indeed result (a report on a major failure that started from incipient cuts along the borders is given in [23].

Of course, further numerical and experimental investigation is required, before more definitive conclusions are proposed, and that will be pursued in future works.
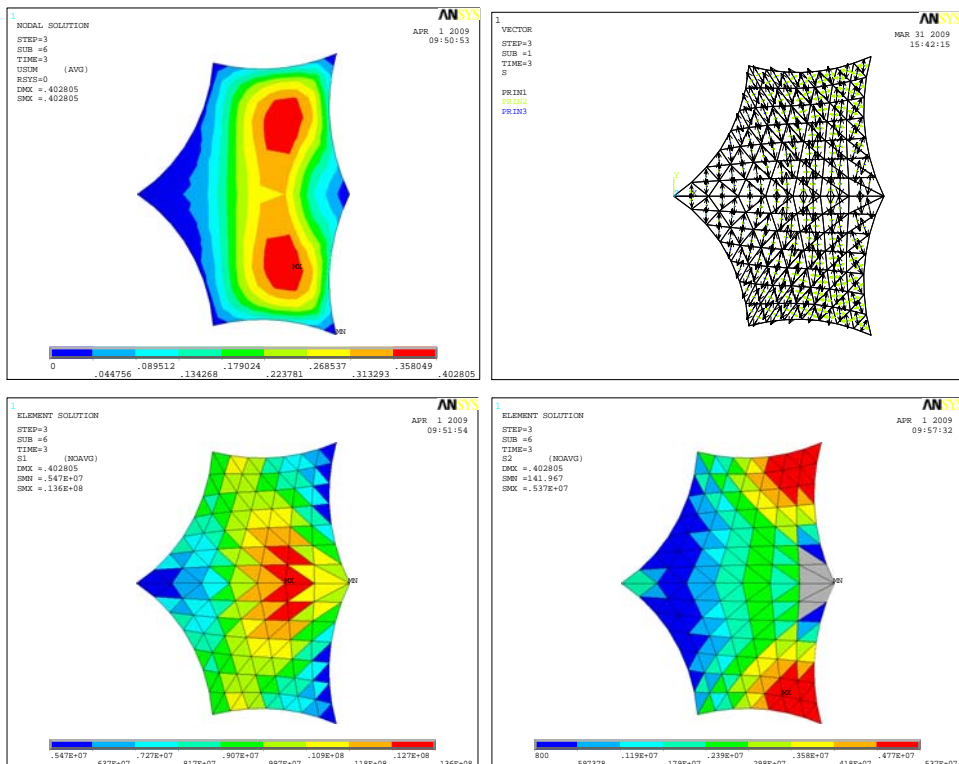

Figure 8: Results for the fully adherent model, solve in Ansys. 1st row: displacement norms and principal stress directions; 2nd row: 1st and 2nd principal stresses.

Table 1. Comparison of selected results	Fully-adherent model			Ideal-sliding model	
	SATS-Newton	*SATS- Relax*	Ansys	SATS-Newton	*SATS- Relax*
Maximum Membrane Displacement [m]	0.40403	0.40343	0.40285	0.46468	0.46605
Maximum 1st Principal Stress σ_I [MPa]	13.60974	13.59338	13.6	26.49613	26.54674
Minimum 2nd Principal Stress σ_{II} [MPa]	0	0	0.000142	0	0
Maximum 2nd Principal Stress σ_{II} [MPa]	5.37598	5.37532	5.37	6.71951	6.73104

Acknowledgement

References

[1]   Sommers J., *Fentress Bradburn Architects´ Gateway to the West: Desgining the Passenger Terminal Complex at Denver International Airport*, The Images Publishing Group Pty Ltd, Victoria, 2000.

[2]   Song C., Analysis of Tensioned Membrane Structures Considering Cable Sliding". *Journal of Zhejiang University SCIENCE* **4** (6), 2003, 672-682.

[3]   Matsumura T., Oda K. and Tachibana E., Finite Element Analysis of Cable Reinforce Membrane Structures with the Use of Bendable-element. *IASS International Symposium on Shell and Spatial Structures*, Singapore, 1997, 567-576.

[4]   Blezinger K.U. and Ramm E., A general finite element approach to the form finding of tensile structures by the updated reference strategy, *Int. J. Numer. Meth. Engnr* **14** (2), 1999, 1231-1259.

[5]   Ishii K., Form finding analysis in consideration of cutting patterns of membrane structures, *Int. J. Space Structures* **14** (2), 1999, 105-120.

[6]   Noguchi H. and Kawashima T., Meshfree analyses of cable-reinforced membrane structures by ALE–EFG method, *Engineering Analysis with Boundary Elements* **28,** 2004, 443–451.

[7]   Aufaure M., A finite element of cable passing through a pulley, *Computer & Structures* **46** (5), 1993, 807–912.

[8]   Pauletti R.M.O and Pimenta P.M., Formulação de Um Elemento Finito de Cabo Incorporando O Efeito do Atrito, in *XV CILAMCE*, 1994, Belo Horizonte, Brazil.

[9]   Pauletti R.M.O. and Pimenta P.M., Formulação de um elemento finito de cabo incorporando o efeito do atrito ('elementos de cabos escorregando'). *Revista Internacional de Métodos Numéricos para Cálculos y Diseño en Ingenieria* **11** (4) , 1995, 565-576

[10] Pauletti R.M.O. and Pimenta P.M., Application of a sliding cable element to the modeling of prestressing tendons. In *Joint Conference of Italian Group of Computational Mechanics and Ibero-Latin American Association of Computational Methods in Engineering*, 1995, Padua, Italy.

[11] Deifeld T.E.C., Pauletti R.M.O., Numerical and physical modeling of tensegrity structures. In *IASS 2004 Symposium - Shell and Spatial Structures: from Models to Realization*, Editions de l'Espérou, Collection Formes-Forces, 2004.

[12] Mitsugi J., Static Analysis of Cable Networks and Their Supporting Structures, *Computers & Structures* **51**, (1), 1992, 47-56.

[13] Zhou B., Accorsi M.L. and Leonard J.W. , Finite Element for Modeling Sliding Cable Elements, *Computers & Structures* **82**, 2004, 271-280.

[14] Pauletti R.M.O., Guirardi D.M. and Deifeld T.E.C., Argyris' Natural Membrane Finite element Revisisted. In *Textile Composites and Inflatable Structures*, Barcelona, CIMNE, 2005, 335-344.

[15] Pauletti R.M.O., Static Analysis of Taut Structures. In *Textile Composites and Inflatable Structures II.* Dorderecht: Springer-Verlag, 2008, 117-139.

[16] Pauletti R.M.O., História, Análise e Projeto de Estruturas Retesadas. Habilitation Thesis (in Portughese). Polytechnic School of the University of São Paulo, 2003.

[17] Aufaure M., A three-node cable element ensuring the continuity of the horizontal tension; a clamp-cable element, *Computer & Structures* **74,** 2000, 243–251.

[18] Martins C.B., *Estudo do efeito do escorregamento dos cabos de borda em estruturas de membrana*. M.Sc. Thesis (in Portughese). Escola Politécnica da Universidade de São Paulo, 2009.

[19] Pauletti R.M.O and Brasil R.L.M.R.F., Structural Analysis and Construction of the Membrane Roof of the "Memorial dos Povos de Belém do Pará". In *II Simposio Latinoamericano de Tensoestructuras,* Caracas, 2005.

[20] Argyris J.H., Dunne P.C., Angelopoulos T., Bichat B. (1974) Large natural strains and some special difficulties due to non-linearity incompressibility in finite elements. *Comp. Meth. Appl. Mech. Eng.* **4** (2), 2007, 219–278

[21] T. Akita *et al*. A simple computer implementation of membrane wrinkle behavior via a projection technique. *Int. J. Numer. Meth. Engnr* 2007 **71**, 1231-1259.

[22] Pauletti R.M.O., Guirardi D.M. and Gouveia S., Modeling sliding cables and geodesic lines through dynamic relaxation, *IASS SYMPOSIUM*, Valence, 2009.

[23] Pauletti R.M.O. *et. al.* Collapse and reconstruction of a large membrane structure in Brazil. In *IASS2007 Shell and Spatial Structures: Structural Architecture Towards the future, looking to the past*, 2007, Venice.